6-30-2022

Transient Thermal Analysis of a Railroad Bearing Adapter for Optimal Placement of Onboard Sensors

Javier E. Arroyo

Constantine Tarawneh

Arturo Fuentes

Roberto A. Garcia

Jose G. Gallegos

Proceedings of the 2022 Joint Rail Conference
JRC2022
April 20-21, 2022, Virtual, Online

JRC2022-78219

TRANSIENT THERMAL ANALYSIS OF A RAILROAD BEARING ADAPTER FOR OPTIMAL PLACEMENT OF ONBOARD SENSORS

Javier E. Arroyo
Mechanical Engineering Department
University of Texas Rio Grande Valley
University Transportation Center for Railway Safety (UTCRS)
Edinburg, TX 78539, USA
javier.arroyo01@utrgv.edu

Constantine Tarawneh, Ph.D.
Mechanical Engineering Department
University of Texas Rio Grande Valley
University Transportation Center for Railway Safety (UTCRS)
Edinburg, TX 78539, USA
constantine.tarawneh@utrgv.edu

Arturo Fuentes, Ph.D.
Mechanical Engineering Department
University of Texas Rio Grande Valley
University Transportation Center for Railway Safety (UTCRS)
Edinburg, TX 78539, USA
arturo.fuentes@utrgv.edu

Roberto A. Garcia
Mechanical Engineering Department
University of Texas Rio Grande Valley
University Transportation Center for Railway Safety
Edinburg, TX 78539, USA
roberto.a.garcia01@utrgv.edu

Jose G. Gallegos
Mechanical Engineering Department
University of Texas Rio Grande Valley
University Transportation Center for Railway Safety
Edinburg, TX 78539, USA
jose.gallegos05@utrgv.edu

ABSTRACT

Bearing temperature serves as an important metric used in identifying defective bearings in the rail industry. Current defect detection systems, such as the Hot Box Detectors (HBDs), are used to measure the temperature of freight car roller bearings. The HBD is a wayside device that utilizes a non-contact infrared sensor to determine the operating temperature of a railroad bearing as it passes over the HBD. Railroads analyze the data collected by HBDs to detect and flag defective bearings. If the operating temperature of a bearing surpasses a predetermined threshold, an emergency stop is initiated, and the bearing is removed from service and sent for inspection. One major drawback of HBDs is that they have been associated with many "false positives," which has resulted in costly train stoppages and delays.

To combat that, researchers have opted to use wireless onboard sensor devices mounted directly on the bearing adapter. One such device is the wireless onboard health monitoring system developed by the University Transportation Center for Railway Safety (UTCRS) that utilizes temperature and vibration sensors to detect the condition of rolling stock. However, because the device is affixed to the bearing adapter and not the bearing itself, the strategic placement of the temperature sensor on the adapter is crucial in minimizing the thermal lag associated with the heat transfer from the bearing to the location where the temperature is measured, as this will directly affect the accuracy of the readings. By conducting a transient heat transfer finite element analysis (FEA), the estimated time-lag and the temperature distribution within the bearing adapter can be determined. To validate the accuracy of the transient FEA model, the results were compared to data acquired from laboratory testing performed on the UTCRS dynamic bearing test rigs. The results obtained in this study can be used to identify optimal anchor points for the temperature sensors on the bearing adapter, and in turn, increase the proficiency of wireless onboard sensor devices in detecting defective components.

Keywords: transient thermal modeling, bearing adapter temperature map, bearing adapter thermal lag, finite element thermal model.

1. INTRODUCTION

One of the leading mechanical causes of derailments in the rail industry is bearing failure. The railroad industry currently utilizes two different types of wayside detection systems to monitor the health of tapered-roller bearings in active service, namely: the Trackside Acoustic Detection Systems (TADS^{TM}) and the wayside Hot-Box Detectors (HBDs). However, these systems come with limitations that can lead to bearings being flagged incorrectly resulting in costly delays due to unnecessary train stoppages. With bearing failures being responsible for approximately 20% of the 800-million-wheel removals, annually, in the North American rail network, this issue is too prevalent to depend on a system with reduced reliability [1].

HBDs use non-contact infrared sensors to measure the temperature radiated from the wheel-axle assemblies as they roll over the detector. The HBD will alert the train operator when any bearings operate at a temperature that is 94.4ºC (170ºF) greater than the ambient temperature or 52.8ºC (95ºF) greater than the temperature of the mate bearing that shares the same axle [2]. However, many railroads have opted to use data acquired from HBDs to identify bearings operating at temperatures that are statistically higher than the average of all bearing temperatures on the same side of the train [3]. These bearings, which are referred to as “warm-trending” bearings, are removed from service and sent to specialized facilities for disassembly and inspection.

HBDs are sparsely installed across North America, which is one of their limiting factors. The North American railroads have installed around 6,000 HBD detectors throughout their network and placed them every 40-rail km (25 miles) to 64-rail km (40 miles) on average [4]. A bearing burnout usually occurs in less than 3 minutes. Hence, a freight car traveling at 60 mph would see the bearing fail over the course of 3 miles. Meaning that, HBDs are too few and far between to be able to proactively detect bearing failures. Detection is further hampered by several factors including environmental conditions, railroad bearing class which determines bearing position on the axle relative to the wayside detector sensor location, surface conditions of the bearing cups (outer rings), and train speed as it passes over the HBDs. Hence, several laboratory and field studies have indicated that the accuracy and reliability of the HBD temperature readings are inconsistent [5].

To combat these limitations, researchers at the University Transportation Center for Railway Safety (UTCRS) have opted to use wireless onboard sensor devices mounted directly on the railroad bearing adapter. This onboard health monitoring system analyzes both the temperature and the vibration profiles of the railroad bearing. However, the wireless onboard monitoring system developed by the UTCRS predicts the bearing operating temperature indirectly from its affixed position on the bearing adapter instead of reading the actual bearing surface temperature. This process introduces a thermal time lag between measured and actual bearing temperature. To understand this thermal delay, a transient heat transfer finite element analysis (FEA) was performed to obtain the thermal distribution throughout the bearing adapter so that an optimal position for measuring temperature could be identified minimizing the associated measurement lag. The FEA simulations were compared against temperature data acquired from experiments conducted on the UTCRS dynamic test rigs to validate the accuracy and reliability of the simulation results.

2. EXPERIMENTAL SETUP AND PROCEDURES

The UTRCS dynamic bearing tester, pictured in Figure 1, was used to perform all relevant experiments for this study. This test rig can accommodate four Class F (6½"×12") or Class K (6½"×9") tapered-roller bearings pressed onto a test axle. A fully loaded railcar applies a load of 153 kN (34.4 kip) per bearing for Class F and K bearings. However, only Class F bearings were used in the experiments carried out for this study. The tester is equipped with a hydraulic cylinder that allows each test bearing to be loaded up to 230 kN (51.7 kips) or 150% of the load experienced by a fully loaded railcar. The data presented in this paper was collected utilizing two loading conditions; namely, 17% load, which represents an empty railcar, and 100% load, which corresponds to a fully loaded railcar.

FIGURE 1: FOUR-BEARING TESTER (4BT)

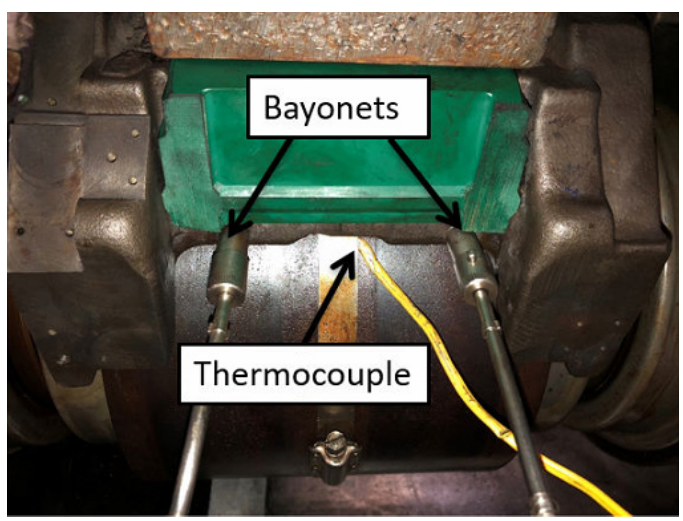

FIGURE 2: THERMOCOUPLE AND BAYONET MEASURING LOCATIONS

The test rig is equipped with a 22 kW (30 hp) variable speed motor which allows the bearings to be tested at different simulated train velocities. For this study, the rotational velocity used was 498 RPM, which is equivalent to a simulated train speed of 85 km/h (53 mph). The bearings were actively air-cooled by three industrial-size fans that produced an average air stream of 6 m/s (13.4 mph). A variable frequency drive (VFD) controlled the motor speed and monitored the motor power consumption.

The test bearings were instrumented with custom accelerometers placed strategically to capture the vibration levels within each bearing. Additionally, each test bearing was instrumented with two K-type bayonet thermocouples, and one regular K-type thermocouple, as pictured in Figure 2. The two bayonet thermocouples recorded temperatures exactly at the centers of the two cup raceways, and the clamped regular thermocouple measured the temperature midway along the width of the bearing cup (outer ring). The bearing operating temperature was obtained by averaging the three temperature readings recorded by the two bayonets and one regular K-type thermocouple. This average cup temperature represented the bearing operating temperature that was systematically compared with the Finite Element Model (FEM) results for optimization and validation of the devised model.

The bearing adapter was modified to accept a regular K-type thermocouple to record the temperature at the location shown in Figure 3. The same exact thermocouple location was also considered in the finite element model. The temperatures from the thermocouple and the FEM were compared to verify the fidelity of the model simulations and to determine the optimal location(s) for the wireless onboard condition monitoring device.

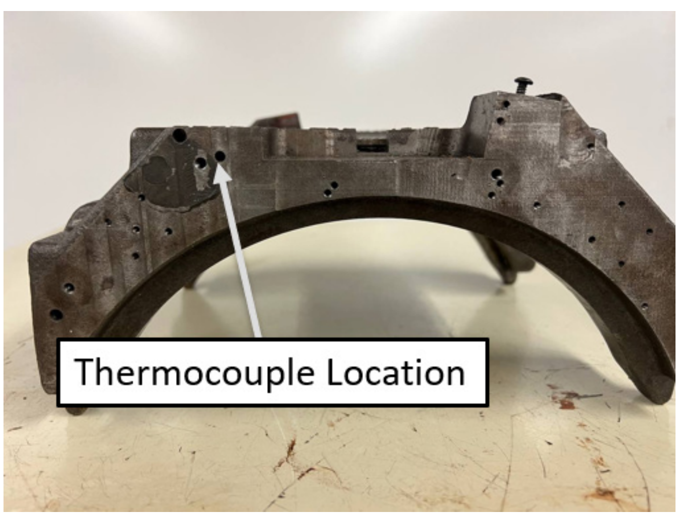

FIGURE 3: BEARING ADAPTER THERMOCOUPLE LOCATION

3. FINITE ELEMENT MODEL (FEM)

An experimentally validated transient finite element thermal model that can be used to obtain temperature distribution maps of complete bearing assemblies in operation is presented hereafter. A computer aided design (CAD) model was created in SolidWorks™ to develop a finite element model (FEM) for the heat transfer analysis. A total of 146,202 mesh elements were used to generate the FEM depicted in Figure 4.

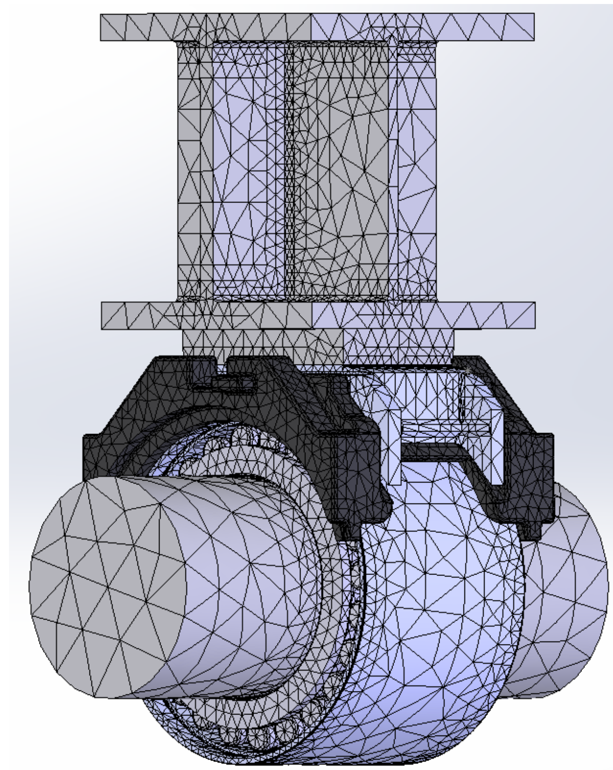

FIGURE 4: LABORATORY TEST RIG FEA MODEL

A combination of brick, pyramid, tetrahedral, and wedge elements were used to successfully mesh the model. The FEM includes a tapered roller bearing that is pressed onto the axle and assumes that all the rollers generate equivalent amounts of thermal load in the system. The length of the axle accounts for the different thermal runways partially caused by the insulating properties of the thermoplastic elastomer suspension pad at the other end of the system. Some boundary conditions and overall heat transfer coefficients were acquired from previous experimental and theorical work [6]. Four major boundary conditions were applied: convection, conduction, heat generation, and heat flux. The model's complexity was reduced by neglecting the presence of bearing cone cages, seals, wear rings, and grease. The thermal resistances of both the grease and the polyamide cages are very large compared to that of the other bearing components, and their exclusion is justified by Tarawneh et al [7]. Because this is a static model, the actual rotation of the cone assembly inside the bearing was not directly simulated but was instead considered by applying an average heat flux through all 46 rollers inside the bearing. The total input motor power was distributed evenly across the four bearings of the 4BT (Figure 1). Since only one bearing was simulated, the input power per bearing was then converted into the individual roller heat flux by dividing it by 46, the total number of rollers within a bearing, and then by the roller surface contact area which is about 33.61 cm^2 (5.21 in^2).

Material properties for the bearing components, axle, I-beam, spacer ring, adapter, and spacer plate were all directly selected from SolidWorks™. AISI 4340 Steel with a thermal conductivity of 44.5 $W \cdot m^{-1} \cdot K^{-1}$ was selected for the bearing components. AISI 1035 Steel with a thermal conductivity of 52 $W \cdot m^{-1} \cdot K^{-1}$ was used for the axle, I-beam, spacer ring, and spacer plate. The properties of the bearing adapter polymer pad material were sourced from BASF literature for thermoplastic polyurethane (TPU) considering grades with the same Shore durometer value. Cast alloy steel was selected for the bearing adapter with a thermal conductivity of 38 $W \cdot m^{-1} \cdot K^{-1}$. Convection coefficient values for all the FEM components are listed in Table 1 with some values obtained from previous related work [8-9].

TABLE 1: CONVECTION COEFFICIENT VALUES FOR EACH FEM COMPONENT

Component	h_{avg} [$W \cdot m^{-2} \cdot K^{-1}$]
I-beam	19.0
Spacer Plate	18.3
AdapterPlus™	17.9
Adapter Pad	17.9
Axle	65.9

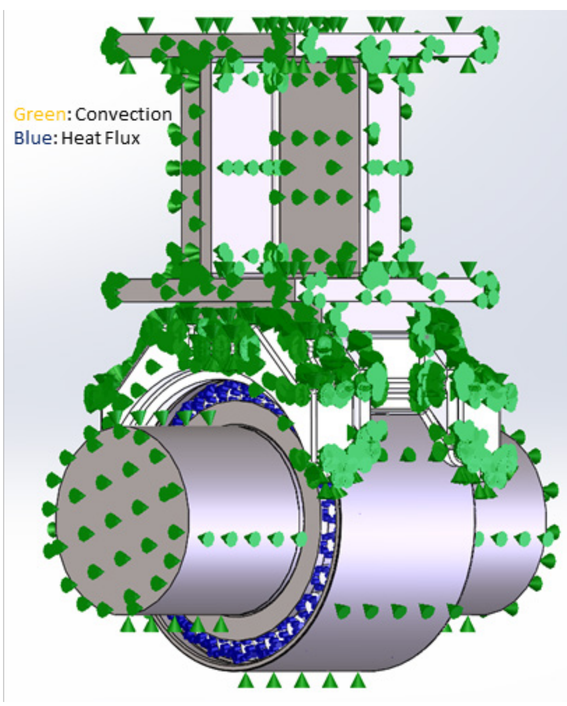

FIGURE 5: BOUNDARY CONDITIONS APPLIED TO EACH COMPONENT

The thermal contact resistance between the adapter and the bearing cup contact surfaces affects the amount of heat transferred from the bearing to the adapter. The thermal contact resistance varies depending on several factors which include the loading conditions of the freight railcar whether it is empty or fully loaded, the type of adapter used, and the condition of the contact surfaces. For example, new bearings and adapters will have clean smooth surfaces which enhances the contact between them and reduces the thermal contact resistance. On the contrary, surfaces of bearings and adapters in rail service will have some roughness to them due to accumulated rust from environmental conditions, which can increase the thermal contact resistance. Based on extensive laboratory dynamic testing performed with old and new adapters for Class F and K bearings under full and empty railcar loads, an average thermal contact resistance of 0.01 $m^2 \cdot K \cdot W^{-1}$ was obtained for the contact surfaces between the bearing cup and adapter. This thermal contact resistance value was applied to the FEM simulations presented in this paper. Figure 5 displays the FEM with the system boundary conditions applied to each component individually. The green markers on Figure 5 signify the applied convection conditions summarized in Table 1, whereas the blue markers denote the applied roller heat flux.

The transient thermal analysis required a time step and a targeted time frame for computational analysis. For this experiment, a time of 10800 seconds (3 hours) was selected, along with a time step of 300 seconds (5 minutes). These criteria are justified for initial FEA model validation.

4. RESULTS AND DISCUSSION

4.1 Experiment 236

Experiment 236 tested four Class F control bearings operating at a simulated train speed of 85 km/h (53 mph). Figure 6 gives the motor power consumption along with the temperature profiles of the test bearing and its adapter during a 12-hour stretch of the experiment.

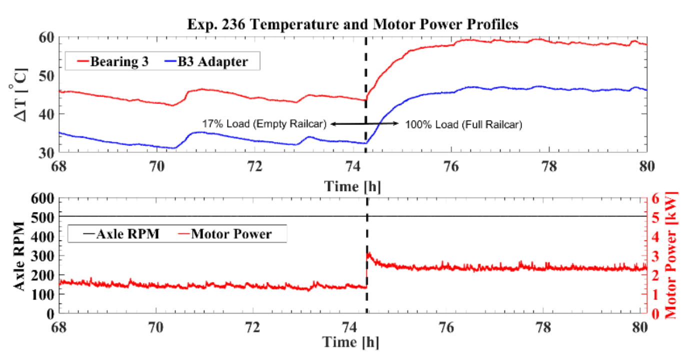

FIGURE 6: TEMPERATURE AND MOTOR POWER PROFILES

Initially, the test bearings were run at an axle rotational speed of 498 RPM, which simulates a train traveling at 85 km/h (53 mph), under 17% load (simulating an empty railcar) to allow the grease to break in. The duration of the break-in period ranges from 1 to 3 days. Once this stage was cleared, the load was increased to 100% load (simulating a fully loaded railcar) while the speed remained at 85 km/h (53 mph). The average ambient temperature in the laboratory was 23ºC (73ºF) which was used to determine the bearing and adapter operating temperatures above ambient. Because all four bearings on the test axle maintained average operating temperatures above ambient of about 59ºC (106ºF) at 85 km/h (53 mph) under full railcar load, the motor power consumption was assumed to be equally distributed among the four test bearings. For FEM validation purposes, the test bearing placed in the B3 axle position, and its adapter were chosen for direct comparison with the FEM simulation results.

As previously mentioned, the heat flux was calculated by obtaining the average motor power at full railcar load and a speed of 85 km/h and dividing it by four, then by 46 rollers, then by the roller surface contact area. The resulting average motor power was 2.34 kW (see Figure 6) which translates into an applied roller heat flux of about 3,784 $W{\cdot}m^{-2}$. The bearing and adapter had initial operating temperatures above ambient of 42.2ºC (76ºF) and 33.0ºC (59ºF), respectively. These initial temperatures were obtained from Figure 6 at the points of intersection of the corresponding temperature profiles with the vertical black dashed line on the graph. The initial bearing and adapter operating temperatures were applied to the FEM along with the rest of the boundary conditions described earlier and the simulation was started. Figure 7 presents the resulting FEM simulation.

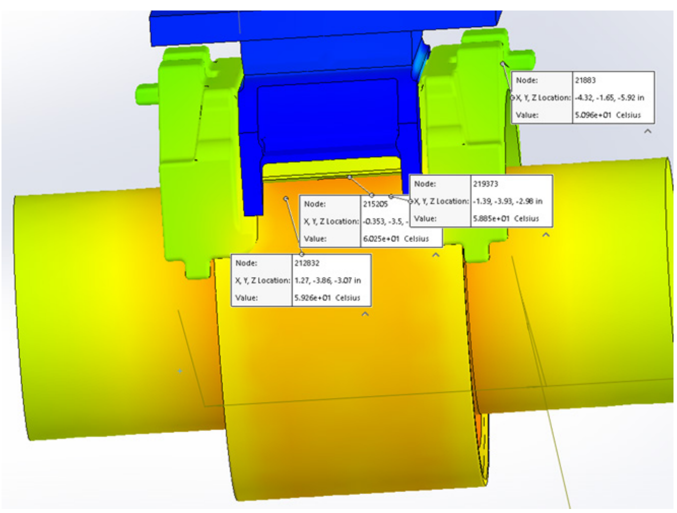

FIGURE 7: FEM SIMULATION RESULTS FOR BEARING AND ADAPTER

The FEM simulation of Figure 7 illustrates the locations where the bearing and adapter operating temperatures were obtained for comparison with the experimentally acquired temperature data. As previously explained, the average bearing operating temperature was calculated by taking the average value of the three thermocouple sensors pictured in Figure 2. The same exact process was followed to obtain the bearing operating temperature from the FEM simulation depicted in Figure 7. Note that the simulation results were expected to be slightly higher due to neglecting the motor power losses in the simulation (e.g., pulley system, frictional heating, etc.). The comparison summaries between the FEM simulation results and the experimental data are presented in Table 2 and Table 3 along with the respective percent error.

TABLE 2: BEARING OPERATING TEMPERATURE COMPARISON SUMMARY

Bearing Operating Temperature			
$R''_{t,c} = 0.01$ [$m^2{\cdot}K{\cdot}W^{-1}$]			
Experimental [°C]	FEM Simulation [°C]	Time [min]	Percent Error [%]
49.0	51.3	30	4.7
52.5	53.9	60	2.7
54.9	55.3	90	0.7
55.7	56.2	120	0.9
56.0	57.0	150	1.8
57.2	57.5	180	0.5

TABLE 3: ADAPTER OPERATING TEMPERATURE COMPARISON SUMMARY

Adapter Operating Temperature			
$R''_{t,c} = 0.01$ [$m^2{\cdot}K{\cdot}W^{-1}$]			
Experimental [°C]	FEM Simulation [°C]	Time [min]	Percent Error [%]
39.8	42.5	30	6.8
43.5	45.0	60	3.4
45.8	46.6	90	1.7
46.6	47.7	120	2.4
47.0	48.3	150	2.8
48.2	48.8	180	1.2

As shown in Table 2 and Table 3, the FEM simulation results fall within 7% of the experimental data. As expected, the first time-step compared to the experimental results will have the highest percent error. This is due to the assumed initial conditions for all the components at the start of the transient finite element model simulation. Small fluctuations in the experimental data are also expected due to roller misalignments and subsequent alignment. Although, looking at the steady-state nature of the motor power profile, it appears that these fluctuations were minimal. After the 30-minute mark, the FEM simulation results fall within 3% of the experimental data. The percent error values listed in Table 2 and Table 3 were calculated using Equation (1),

$$\delta = \left|\frac{Experimental - FEM}{Experimental}\right| \times 100 \tag{1}$$

Figure 8 is a visual representation of the data summarized in Table 2 and Table 3. As explained earlier, unlike the smooth FEM simulation results which assume ideal operating conditions (i.e., no power losses or variations), the experimental temperatures show a slight variance caused by roller dynamics.

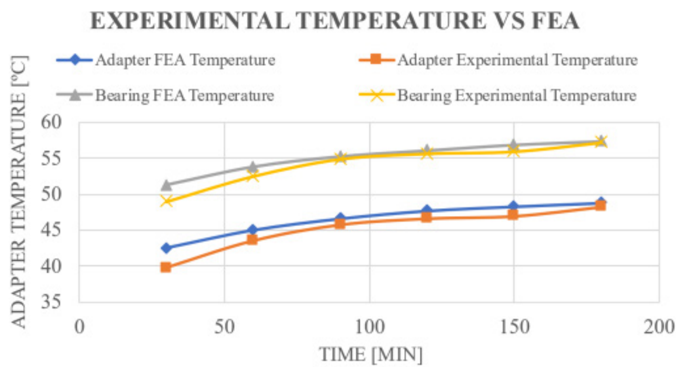

FIGURE 8: EXPERIMENTAL TEMPERATURES VERSUS FEM SIMULATION RESULTS

5. CONCLUSIONS

Railroad bearings may be removed from service for several reasons which include triggering a wayside detection system or as part of an entire wheel-axle replacement due to a wheel defect. Current wayside condition monitoring systems are reactive in nature in that they normally detect defective bearings operating above predetermined thresholds. This process leaves room for error where failing bearings that do not meet these thresholds can be overlooked. Hot-Box Detectors (HBDs) solely rely on temperature measurements and are not effective at identifying defective bearings at their early stages of deterioration since the operating temperature of these bearings is usually within that of defect-free (healthy) bearings.

The shortcomings of the wayside detection systems have prompted the slow shift to onboard sensors. With that in mind, the University Transportation Center for Railway Safety (UTCRS) developed a wireless onboard condition monitoring sensor module which actively monitors the temperature and vibration levels of a bearing from its affixed position on the corresponding bearing adapter. However, since the temperature measured by the sensor is that of the adapter and not the bearing itself, a thermal lag is present. This lag is apparent in Figure 6 where a sudden change in motor power is not immediately accompanied by a corresponding rise in operating temperature. Instead, due to the thermal lag, the operating temperature increases over a longer period. Finite Element Models (FEM) with appropriate boundary conditions were devised to simulate this thermal response in both Class F and Class K railroad bearings. The experimental data presented in this paper is for Class F bearings. The resulting FEM simulation provided the temperature distribution, illustrated in Figure 7, which contrasts the operating temperatures of the bearing and its adapter. The finite element analysis (FEA) revealed that the adapter temperature distribution was mostly uniform, which means that the bearing adapter can be treated as a lumped capacitance body. Moreover, this also implies that the wireless onboard sensor module can be placed anywhere the adapter geometry permits. To fully rely on the FEM, more simulations must be systematically compared to experimental data taken under different operating conditions for a larger set of healthy and defective bearings. Doing so will increase the reliability and efficacy of the devised FEM and will minimize the percent error between the numerical and experimental results.

ACKNOWLEDGMENTS

This study was made possible through funding provided by the University Transportation Center for Railway Safety (UTCRS) and the Dwight David Eisenhower Transportation Fellowship Program (DDETFP) through a USDOT Grant No. 693JJ32245180.

REFERENCES

[1] Voestalpine, "Phoenix MB Intelligent Rolling Stock Monitoring, Hot Box and Wheel Detection with Multi Beam Technology," *Voestalpine Signaling*, Germany, 2014.

[2] T. Sultana and L. Stabler, "Condition-Based Maintenance with Detectors," in IHHA, Perth, Australia, 2015

[3] Karunakaran, S., and Snyder, T.W., "Bearing Temperature Performance in Freight Cars," *Proceedings Bearing Research Symposium, sponsored by the AAR Research Program in conjunction with the ASME RTD Fall Conference*, Chicago, IL, September 11-12, 2007.

[4] H. Wang, T.F. Conry, C. Cusano, "Effects of Cone/Axle Rubbing Due to Roller Bearing Seizure on the Thermomechanical Behavior of a Railroad Axle," *Journal of Tribology*, Vol. 118, pp. 311-319, 1996.

[5] Tarawneh, C., Aranda, J., Hernandez, V., et al., "An Investigation into Wayside Hot-Box Detector Efficacy and Optimization," *International Journal of Rail Transportation,* Vol. 8(3), pp. 264-284, 2020.

[6] Mealer, A., Tarawneh, C., Crown, S., "Radiative Heat Transfer Analysis of Railroad Bearings for Wayside Hot-box Detector Optimization," *Proceedings of the Joint Rail Conference*, Philadelphia, PA, April 4-7, 2017.

[7] Tarawneh, C., Cole, K., Wilson, B.M., Alnaimat, F., "Experiments and Models for the Thermal Response of Railroad Tapered-Roller Bearings," *International Journal of Heat and Mass Transfer*, Vol. 51, pp. 5794-5803, 2008.

[8] Tarawneh, C., et al., "Thermal Modeling of a Railroad Tapered-Roller Bearing Using Finite Element Analysis," *Journal of Thermal Science and Engineering Applications*, Vol. 4(3), pp. 9-19, 2012.

[9] Zagouris, A., Fuentes, A. A., Tarawneh, C., Kypuros, J. A., and Arguelles, A. P., "Experimentally Validated Finite Element Analysis of Railroad Bearing Adapter Operating Temperatures," *Proceedings of the ASME IMECE Conference*, IMECE2012-88639, Houston, TX, November 9-15, 2012.